International Journal of Scientific Research in Mathematical and Statistical Sciences
Vol.**11**, Issue.**6**, pp.**66-74**, December **2024**
E-ISSN: 2348-4519
Available online at: www.isroset.org

Research Article

Unsteady MHD Blood Flow Through Bifurcated Arteries with Heat Source and Magnetic Field in the Presence of Soret Effect

Auwalu Alhassan Girema[1], Yusuf Ya'u Gambo[2], Bashir Yau Haruna[3]

[1,2,3]Dept. of Mathematics, Yusuf Maitama Sule university, Kano, Nigeria

**Corresponding Author: giremaguyuk4321@gmail.com*

Received: 23/Oct/2024; **Accepted**: 25/Nov/2024; **Published**: 31/Dec/2024

Abstract— This study explores unsteady blood flow in bifurcated arteries influenced by a constant transverse magnetic field and heat source. For easy analysis of axial velocity, temperature distribution, concentration of blood component and normal velocity, complex partial differential equations are transformed into ordinary differential equations by the method of separation of parameters subject to the conditions defined. Analytical solution illustrates how varying factors such as Hartmann number (*Ha*), Prandtl number (*Pr*), Schmidt number (*Sc*), Soret parameter (*Sr*) and Decay parameter (λ) affect blood flow dynamics. The analysis was made using Matlab and the results are presented graphically for better understanding.

Keywords— The Blood Flow, Bifurcated Artery, Soret effect, Heat Source, Magnetic Field, Decay parameter.

Table 1. Nomenclature

Nomenclature			
P	Density of blood	K_t	Coefficient of thermal conductivity
M	Dynamic viscosity of the blood (constant)	C_p	Specific heat at constant pressure
P	Pressure of blood	Q	Quantity of heat
σ	Electrical conductivity of the blood	θ	Temperature distribution
B_o	Intensity of the magnetic field	φ	Concentration
G	Gravitational acceleration	Pr	Prandtl number
B	Coefficient of volume expansion due to temperature	Sc	Schmidt number
β'	Coefficient of volume expansion due to concentration	Sr	Soret parameter
T	Temperature of blood	Ha	Hartmann number
T_o	Temperature of the wall (fixed temperature)	τ	Kinematic viscosity
λ	Decay parameter		

1. Introduction

Numerous studies have explored blood flow dynamics and the impact of magnetic fields on physiology of fluids, particularly blood, owing to its electrical conductivity. This interaction, described through magnetohydrodynamics (MHD), has shown potential for treating cardiovascular diseases and related circulatory conditions. Researchers have investigated various mathematical models to understand blood flow behavior under external magnetic influences.

Authors such as Tzirtzilakis [1], Ramamurthy and Shanker [2], Das and Saha [3], and others have investigated blood flow characteristics, especially in narrow channels or through porous media, under the effect of transverse magnetic fields. These studies consider factors like periodic body acceleration, lubricating layers, variable viscosity, and heat transfer in biological systems. The current study extends the work of Islam [4], in which a mathematical model of unsteady blood flow through parallel plate channel under the action of an applied constant transverse magnetic field is proposed. Singh and Rathee [5] provided a precise solution for a two-dimensional blood flow model with changing viscosity within a narrowed artery affected by the presence of low-density lipoproteins in a magnetic field. Their study highlights that individuals with hypertension may be more susceptible to heart circulatory issues. Additionally, Dulal and Ananda [6] examined the influence of a consistent transverse magnetic field on the pulsating movement of blood through a symmetrically shaped tube. Meanwhile, Zamir and Roach [7]

focused on analyzing blood flow after a two-dimensional division with an even, continuous flow. The idea of electromagnetic fields in medical research was firstly given by Kolin [8] and later Korchevskii et al. [9] discussed the possibility of regulating the movement of blood in human system by applying magnetic field. Usman and Mohyud Din [10] proposed their studies on blood flow with nano suspensions flowing through a porous vessel and heat transfer in presence of magnetic field. Tripathi [11] suggested in his study that inclined magnetic field provides modified blood flow results. Allwood and Burry [12] provided effects of heat transfer on blood flow in different parts of the body. Ogulu and Abbey [13] have analyzed the simulation of heat transfer on an oscillatory blood flow in an indented porous artery. Allwood and Burry [14], and Charm et al. [15] experimentally investigated heat transfer in small tubes of diameter 0.6mm in a water bath, while Victor and Shah [16] computed heat transfer for uniform heat flux and uniform wall temperature cases for fully developed flow and in the entrance region. Haldar [17] and Vardanyan [18] conducted studies on blood flow, treating blood as a Newtonian fluid. Varshney et al. [19] explored the effects of a magnetic field on blood flow through arteries with multiple stenoses. Jha and Gambo [20,21,22,23] presented a comprehensive analytical study of Soret and Dufour effects for time-dependent free convection flow in different geometries. Isah et. al. [24] provided analytical and numerical solutions addressing transient magnetohydrodynamic free convection flow in a vertical channel, accounting for the presence of the Soret effect, Dufour effect, thermal radiation, and magnetic field. However, the effects of Soret and Dufour on unsteady MHD blood flow through bifurcated arteries have not been studied.

The aim of this paper is to provide an analytical study of Soret effect (The ratio of thermal coefficient to diffusion coefficient) on unsteady MHD blood flow through bifurcated arteries. The study provides analytical expressions for axial velocity, temperature distribution, concentration of blood component and normal velocity, considering the same boundary conditions as Islam [4]. The study build on the work of Islam [4] by considering Soret effect. The investigation focuses on understanding the impact of Hartmann number (*Ha*), heat source parameter (*S*), Schmidt number (*Sc*), Soret parameter (*Sr*), Decay parameter (λ) and Prandtl number (*Pr*) on blood flow dynamics. This model seeks to simplify the understanding of blood flow behavior, benefiting those involved in physiological fluid dynamics research and medical practice.

1.1 Problem Formulation

The natural blood circulation system comprises elastic tubes with three-dimensional structures, varying cross-sections, and bifurcation angles. However, for mathematical ease, a two-dimensional bifurcation model resembling the geometry proposed by Islam [4] was chosen, allowing analysis of heat effects on unsteady blood flow dynamics. In this study, blood is assumed to be Newtonian, incompressible, homogeneous, and viscous, flowing through a non-conductive parallel plate channel from the main trunk to the branches (see Figure 1 and 2). The mass flow rate perpendicular to the flow direction is represented as (m=2bϱV), where V stands for mean flow velocity, b is the branch diameter, and ϱ is the blood density. For simplicity, the bifurcation angle is assumed to be zero, leading to a division of a parallel stream into two. Additionally, the wall thickness at the bifurcation is deemed negligibly small, allowing the mass flow rate in a cross-section of the branched channel to be represented as m/2. Due to the considerably larger breadth of the channel (parallel to the large artery and larger than 1mm) the blood viscosity is treated as constant throughout this analysis, disregarding the Fahreus-Lindquist effect.

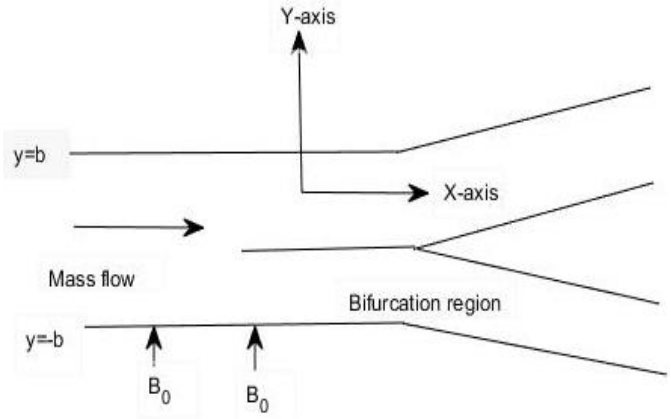

Figure 1. Diagram indicating angle of bifurcation not zero

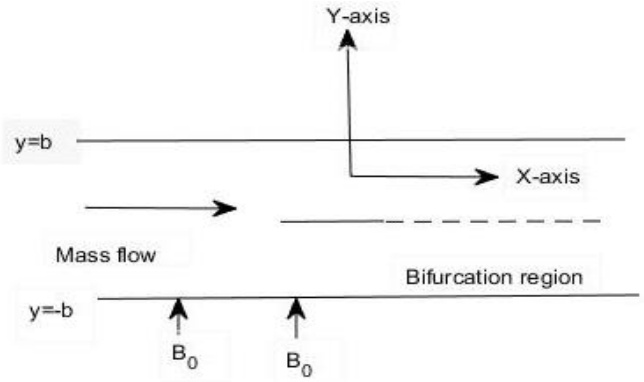

Figure 2. Diagram indicating angle of bifurcation equal to zero

2. Related Work

This work is build on Islam [4] and the concept used is in line with the other literature that appears in the paper.

3.1 Theory/Calculation

$$\frac{\partial u*}{\partial t*}+\frac{1}{\rho}\frac{\partial p*}{\partial x*}=\frac{\mu}{\rho}\frac{\partial^2 u*}{\partial y*^2}-\frac{\sigma B_0{}^2}{\rho}u^*+g\beta(T-T_0)^*+g\beta(C-C_0)^* \quad (1)$$

$$\frac{\partial u*}{\partial x*}+\frac{\partial v*}{\partial y*}=0 \quad (2)$$

$$\frac{\partial T*}{\partial t*}=\frac{K\_t}{\rho C\_p}\frac{\partial^2 T*}{\partial y*^2}+\frac{Q}{\rho Cp}(T-T_0)* \quad (3)$$

$$\frac{\partial C*}{\partial t*}=D\frac{\partial C*}{\partial y*}+Sr*\frac{\partial^2 T*}{\partial y*^2} \quad (4)$$

Non-dimensional variables are defined as follows
$x = \frac{x^*}{b}$, $u = \frac{u^*}{(m/(2b\rho))}$, $h(x,t) = (dp^*/dx^*) / (\eta m / (2b^3\rho))$,
$\tau=\mu/\rho$, $y = \frac{y^*}{b}$, $v = v^*/(m / (2b\rho))$, $t = t^*/(b^2\rho/\eta)$,
$\theta=\theta^*(2b^3\rho^2)/(m\mu)$, $Sr = Sr^*/D$, $\varphi = \varphi^*(2b^3\rho^2) / (m\mu)$ (5)
Substituting Equation (5) into Equations (1)-(4) we have

$$\frac{\partial u}{\partial t} + h = \frac{\partial^2 u}{\partial y^2} - Ha^2u + g\beta\theta + g\beta'\phi \quad (6)$$

$$\frac{\partial u}{\partial x} + \frac{\partial v}{\partial y} = 0 \quad (7)$$

$$\frac{\partial \theta}{\partial t} = (1/\tau Pr)\frac{\partial^2 \theta}{\partial y^2} + (S/\tau Pr)\theta \quad (8)$$

$$\frac{\partial \phi}{\partial t} = (1/Sc)\frac{\partial^2 \phi}{\partial y^2} + (Sr/Sc)\frac{\partial^2 \theta}{\partial y^2} \quad (9)$$

Looking into Equation (8) we observe that the temperature distribution has 1st order derivative in time (t), from this observation we can use the method of separation of parameters on the equation and the solution will be in the following form:

$$\theta = H(y)\, e^{-\lambda^2 t} \quad (10)$$

$$\phi = I(y)\, e^{-\lambda^2 t} \quad (11)$$

$$u = F(y)\, e^{-\lambda^2 t} \quad (12)$$

$$v = G(y)\, e^{-\lambda^2 t} \quad (13)$$

With the help of observations in the previous section, the boundary conditions can be chosen as follows.

u = e^(-λ²t), v = e^(-λ²t), θ = e^(-λ²t), ϕ = e^(-λ²t) at y = -1 (14)

u = 0, v = 0, θ = 0, ϕ = 0 at y = 1 (15)

Substituting Equations (10)-(13) into Equations (6)-(9) we get the following equations

Here are the equations in a Microsoft Word document format:

$$\frac{\partial^2 H}{\partial y^2} + (S + \lambda^2\tau Pr)H = 0 \quad (16)$$

$$\frac{\partial^2 I}{\partial y^2} + Sc\lambda^2 I = -Sr\frac{\partial^2 H}{\partial y^2} \quad (17)$$

$$\frac{\partial^2 F}{\partial y^2} + (\lambda^2 - Ha^2)F = \hbar - g\beta H - g\beta' I \quad (18)$$

G = B (Constant)
(19)

Where $\hbar = \frac{h}{e^{-\lambda^2 t}}$

The boundary conditions defined in Equation (14)-(15) are transformed using Equations (10)-(13) to

F = 1, H = 1, I = 1 at y = -1 (20)

F = 0, H = 0, I = 0 at y = 1 (21)

3.2 Solution to the Problem

From Equation (16)
Let $\Omega = \sqrt{(S + \lambda^2 \tau Pr)}$

$$H = \frac{\cos(\Omega y)}{2\cos(\Omega)} - \frac{\sin(\Omega y)}{2\sin(\Omega)} \quad (22)$$

Using Equation (22), the temperature distribution is given by

$$\theta = \left[\frac{\cos(\Omega y)}{2\cos(\Omega)} - \frac{\sin(\Omega y)}{2\sin(\Omega)}\right] e^{-\lambda^2 t} \quad (23)$$

From Equations (17) and (22) we have

$$I = \left[1 - \frac{(\Omega^2 Sr)}{(Sc\lambda^2 - \Omega^2)}\right]\frac{\cos(\lambda\sqrt{Scy})}{(2\cos(\lambda\sqrt{Sc}))} - \left[1 - \frac{(\Omega^2 Sr)}{(Sc\lambda^2 - \Omega^2)}\right]\left[\frac{\sin(\lambda\sqrt{Scy})}{(2\sin(\lambda\sqrt{Sc}))}\right] + \left[\frac{(\Omega^2 Sr)}{2(Sc\lambda^2 - \Omega^2)}\cos\Omega\right)]\cos(\Omega y) \quad (24)$$

It can be deduced from Equation (24) that the concentration of blood component is given by

$$\phi = \{[1 - \frac{(\Omega^2 Sr)}{(Sc\lambda^2 - \Omega^2)}]\,[\frac{\cos(\lambda\sqrt{Scy})}{(2\cos(\lambda\sqrt{Sc}))}] - [1 - \frac{(\Omega^2 Sr)}{(Sc\lambda^2 - \Omega^2)}]\,[\frac{\sin(\lambda\sqrt{Scy})}{2\sin(\lambda\sqrt{Sc})}] + [\frac{(\Omega^2 Sr)}{(2(Sc\lambda^2 - \Omega^2)\cos\Omega)}]\cos(\Omega y) - [\frac{(\Omega^2 Sr)}{(2(Sc\lambda^2 - \Omega^2)\sin\Omega)}]\sin(\Omega y)\}\, e^{-\lambda^2 t} \quad (25)$$

Using Equations (22) and (24) and letting
$\xi = \sqrt{(\lambda^2 - Ha^2)}$, $\alpha = [\frac{1 - (\Omega^2 Sr)}{(Sc\lambda^2 - \Omega^2)}]$, and $\Omega = \sqrt{(S + \lambda^2 \tau Pr)}$.

$$u = \{[1 - 2(\frac{\hbar}{\xi^2}) + (\frac{g\beta}{(\xi^2 - \Omega^2)}) + (\frac{g\beta\prime\alpha}{2(\xi^2 - \lambda^2 Sc)}) + (\frac{g\beta\prime\Omega^2 Sr}{(\xi^2 - \Omega^2)(Sc\lambda^2 - \Omega^2)})]\,[\frac{\cos(\xi y)}{(2\cos\xi)}] - [1 + (\frac{g\beta}{(\xi^2 - \Omega^2)}) + (\frac{g\beta\prime\alpha}{(\xi^2 - \lambda^2 Sc)}) + (\frac{g\beta\prime\Omega^2 Sr}{(\xi^2 - \Omega^2)(Sc\lambda^2 - \Omega^2)}]\,[\frac{\sin(\xi y)}{(2\sin\xi)}] + (\frac{\hbar}{\xi^2}) - (\frac{g\beta}{2(\xi^2 - \Omega^2)\cos\Omega})\cos(\Omega y) + (\frac{g\beta}{2(\xi^2 - \Omega^2)\sin\Omega})\sin(\Omega y) - (\frac{g\beta'\alpha\cos(\lambda\sqrt{Sc})}{(2(\xi^2 - \lambda^2 Sc)}))\cos(\lambda\sqrt{Scy}) + (\frac{g\beta'\alpha\sin(\lambda\sqrt{Sc})}{(2(\xi^2 - \lambda^2 Sc)})\sin(\lambda\sqrt{Scy}) - (\frac{g\beta'\Omega^2 Sr(\cos\Omega)}{2(\xi^2 - \Omega^2)(Sc\lambda^2 - \Omega^2)})\cos(\Omega y) + \frac{g\beta'\Omega^2 Sr(\sin\Omega)}{2(\xi^2 - \Omega^2)(Sc\lambda^2 - \Omega^2)})\sin(\Omega y)\}\, e^{-\lambda^2 t} \quad (26)$$

Lastly, the normal velocity is obtained from Equation (19) as

$$v = B\, e^{-\lambda^2 t} \quad (29)$$

4. Results and Discussion

This analysis yields theoretical outcomes including the axial velocity, normal velocity, concentration of blood component and temperature distribution within the blood. It is worth noting that setting the Soret parameter and the coefficient of volume expansion due to concentration to be zero (i.e., Sr=0, β'=0), the solution in this paper correspond to those presented

by Islam [4]. The numerical solutions for axial and normal velocity as well as temperature and concentration are graphically presented across varying values of the Hartmann number (*Ha*), Prandtl number (*Pr*), Soret parameter (*Sr*), Decay parameter (λ) and heat source parameter (*S*) against *y*, enhancing comprehension of the scenario.

4.1.1 Temperature for Different Values of Heat Source and Prandtl Number

In Figure 2, we examine the temperature distribution changes concerning *y* at λ=0.5, τ=0.5, *Pr*=1 and *t*=1 for various values of the heat source parameter (*S*=0,1.00,1.25,1.50,1.75,2.00). Notably, for a fixed *y* value, the temperature field escalates with higher values of the heat source parameter. Moreover, the temperature field rises, reaching its peak towards the middle of the channel and subsequently declines. Also, in Figure 3, the Temperature field shows the same behaviour with different values of Prandtl number (*Pr*=0.5,1.00,3.00,5.00,7.00) but the temperature reaches it peak at around *y*=−0.2.

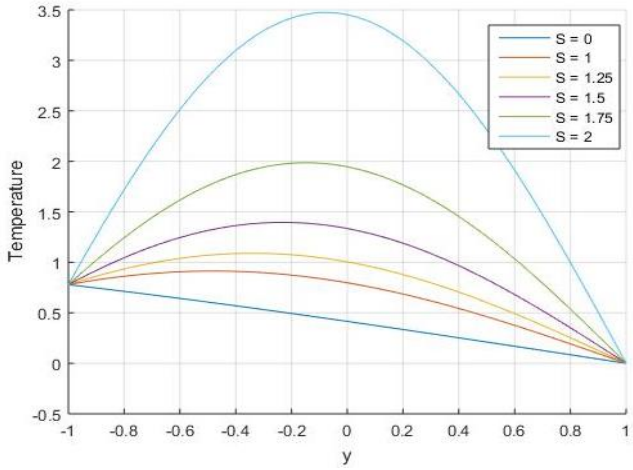

Figure 3. Temperature variation with heat source (S)

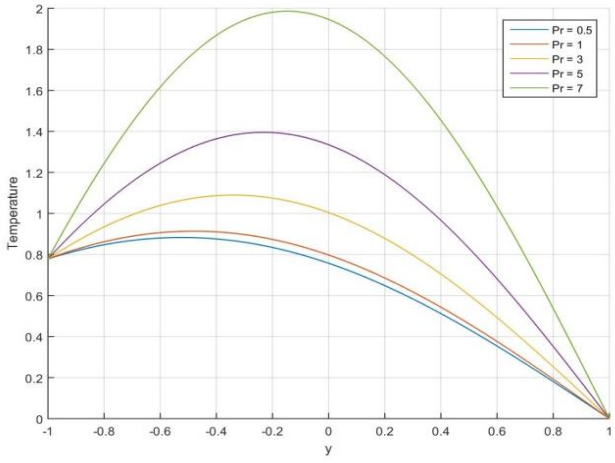

Figure 4. Temperature variation with heat Prandtl Number (Pr)

4.1.2 Temperature for Different Values of Decay Parameter and Kinematic Viscosity

The analysis reveals that the temperature field in Figure 4 experiences a decrease with an increasing decay parameter. The most significant impact of the decay parameter on the temperature field occurs at *y*=-1, while there is almost no effect of the decay parameter on the temperature distribution at *y*=1. Also, in Figure 5, the kinematic viscosity serves as a significant indicator, exhibiting a proportional relationship with blood temperature. As the kinematic viscosity increases, the blood temperature rises in tandem. This correlation is most notable at the midpoint of the artery, reaching a peak temperature before gradually subsiding. The dynamics between kinematic viscosity and blood temperature provide insights into the fluid behavior within the artery, emphasizing a distinctive pattern of temperature variation along the arterial path.

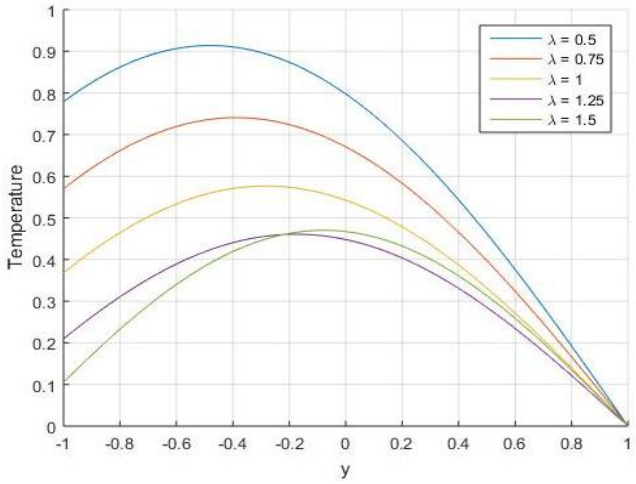

Figure 5. Temperature variation with decay parameter (λ)

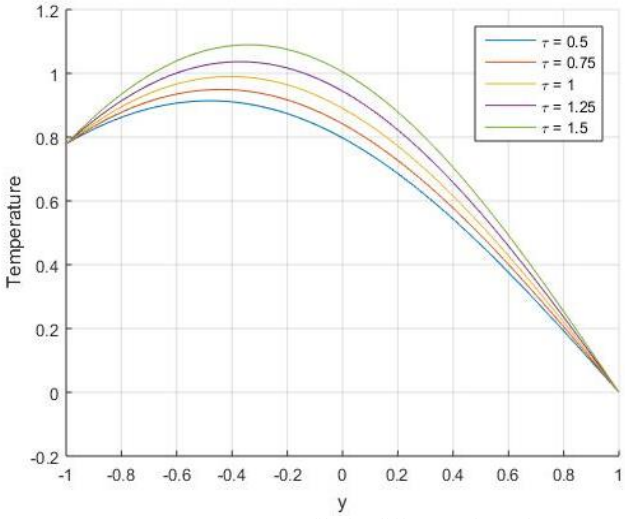

Figure 6. Temperature profile for different values of τ

4.1.3 Tempareture for Different Values of Time

The temperature difference observed in Figure 6 is consistent for equal intervals of time. As time passes, the temperature changes by a constant amount during each successive interval. This proportional relationship signifies a steady and predictable pattern in the evolution of temperature over time.

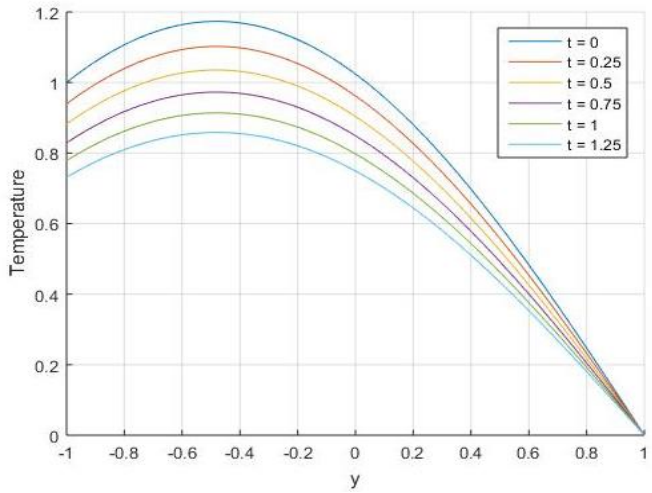

Figure 7. Temperature profile for different values of *t*

4.1.4 Concentration for Different Value of Soret Parameter

In Figure 7, it is evident that the concentration of a blood component near a bifurcation region undergoes a substantial elevation as the Soret parameter increases. This finding is particularly relevant to cardiovascular health, suggesting that variations in the Soret parameter significantly influence blood composition near bifurcation regions. Notably, a more pronounced concentration rise occurs within the range of *Sr*=1.6 to *Sr*=3.5, indicating a critical threshold that may have implications for cardiovascular diseases and the understanding of blood flow dynamics.

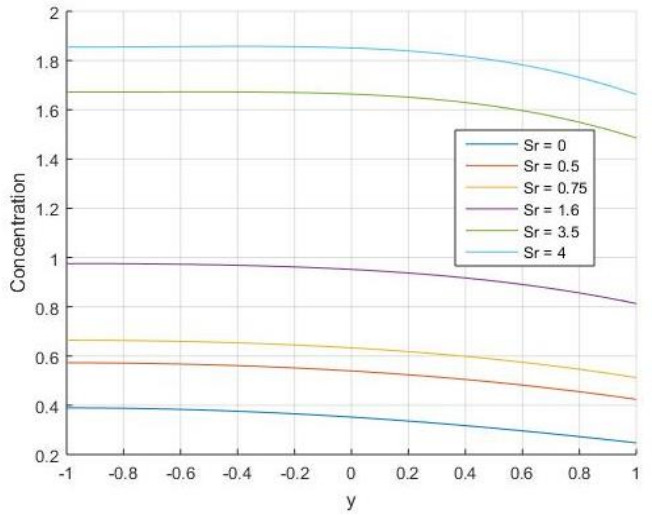

Figure 8. Concentration for different values of *Sr*

4.1.5 Concentration for Different Values of Heat Sources and Decay Parameter

Figure 8 reveals that, the concentration exhibits a minor increase with an increasing value of the heat source. However, a more noticeable rise is observed in the concentration between *y*=−1 to *y*=0.6. Also, in Figure 9, the analysis reveals that the Concentration experiences a decrease with an increasing decay parameter. The significant decrease in concentration occurs as the value of *y* increases.

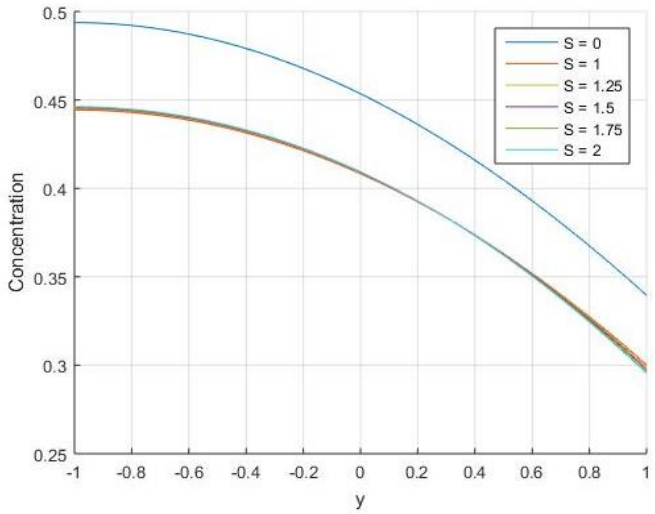

Figure 9. Concentration for different values of *S*

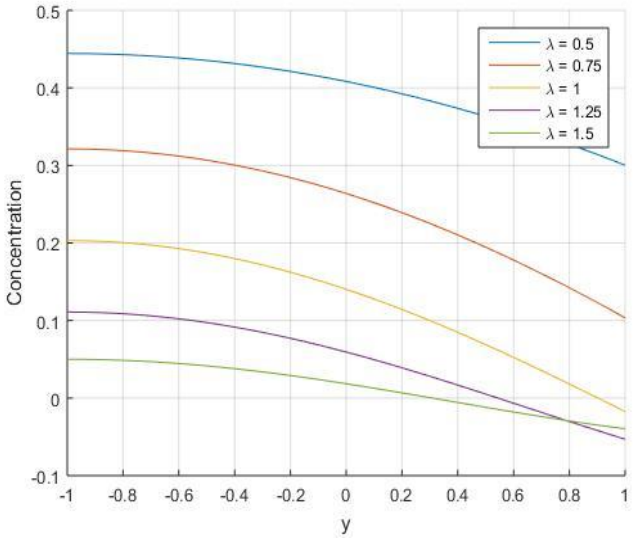

Figure 10. Concentration for different values of λ

4.1.6 Concentration for Different Values of Prandtl Number and Schmidt Number

The concentration shows no significant change with respect to the Prandtl number as observed in Figure 10. However, there is a noticeable sudden decrease in concentration as the value of *y* increases. Figure 11 shows the impact of Schmidt number is irregular, nevertheless, the concentration exhibits a gradual decline from *y*=−1 to *y*=−0.8 followed by a sudden and significant decrease towards the opposite boundary. This irregularity in the Schmidt number's influence suggests a non-uniform pattern in how it affects the concentration distribution. The concentration's nuanced behavior, characterized by a subtle reduction followed by a more pronounced decrease, highlights the complex interaction between the Schmidt number and concentration across the specified range.

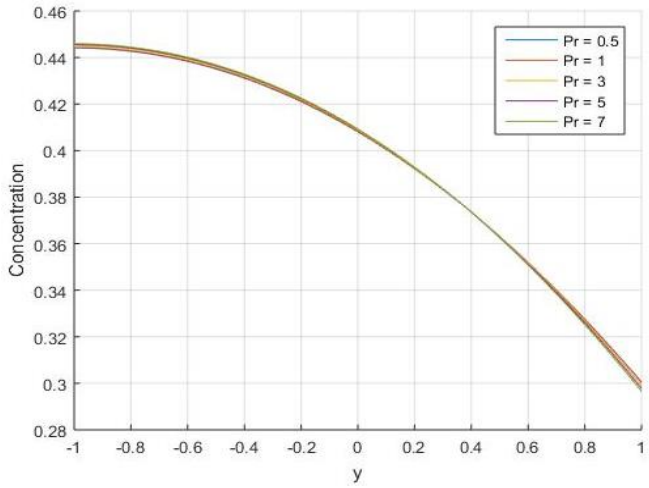

Figure 11. Concentration for different values of *Pr*

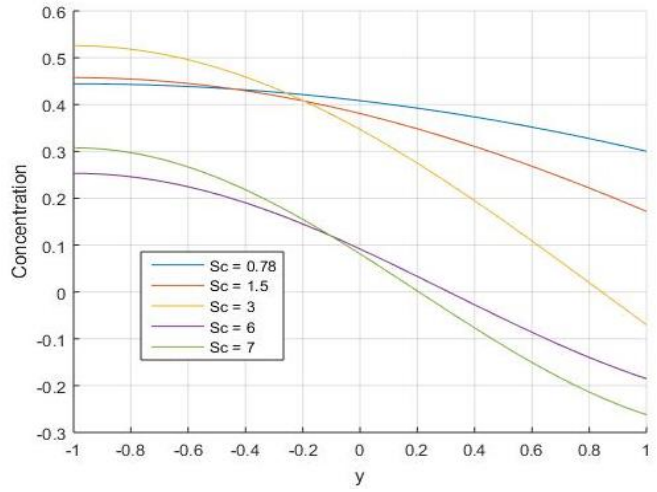

Figure 12. Concentration for different values of *Sc*

4.1.7 Concentration for Different Values of Time

Figure 12, shows that, the rate of concentration change exhibits proportionality with time, meaning that equal time intervals result in consistent temperature differences. Additionally, at t=0, the concentration is higher compared to t values greater than zero. This emphasized that initially, the blood component concentration is elevated, and over time, the body gradually absorbs the concentration, leading to a decrease in concentration as time progresses.

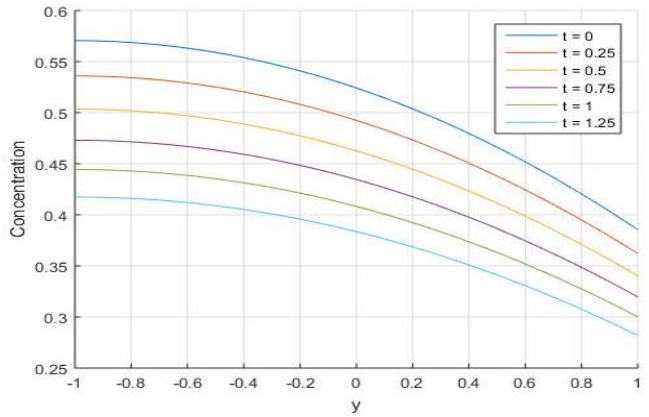

Figure 13. Concentration for different values of *t*

4.1.8 Axial Velocity for Different Values of Soret Parameter

As the Soret parameter increases in Figure 13, there is a noteworthy decrease in blood velocity, demonstrating a substantial impact, especially within the range of Sr=1.6 to Sr=3.5. This observation holds significant implications for cardiovascular health, suggesting that variations in the Soret parameter exert a considerable influence on blood velocity. The wide-ranging effects observed within the specified Sr values highlight a critical range where alterations in blood flow dynamics may occur, providing valuable insights into potential cardiovascular conditions associated with changes in the Soret parameter.

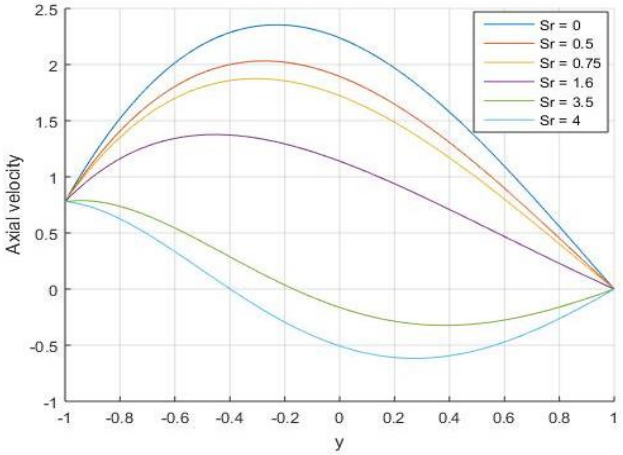

Figure 14. Velocity profile for different values of *Sr*

4.1.9 Axial velocity for Different Value of Prandtl and Schmidt Number

Figure 14 depicts the impact of the Prandtl number on the axial velocity distribution at λ=0.5, μ=0.5, t=1, h=0.5, Ha=1, g=9.81, β=0.5, β'=0.5, Sc=0.78, Sr=0.15. The illustration reveals a rise in axial velocity with an increase in the Prandtl number. Figure 15 depicts the impact of the Schmidt number on the axial velocity distribution at λ=0.5, μ=0.5, Pr=1, S=1, τ=0.5, t=1, h=0.5, Ha=1, g=9.81, β=0.5, β'=0.5, S=1, τ=0.5, Sr=0.15. The illustration reveals a rise in axial velocity with an increase in the Schmidt number.

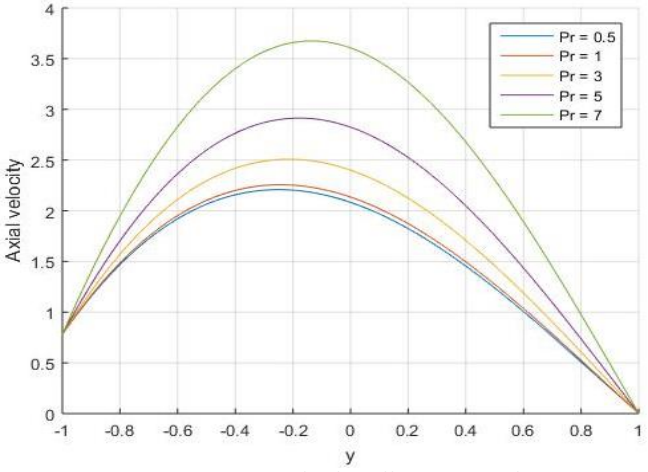

Figure 15. Velocity profile for different values of *Pr*

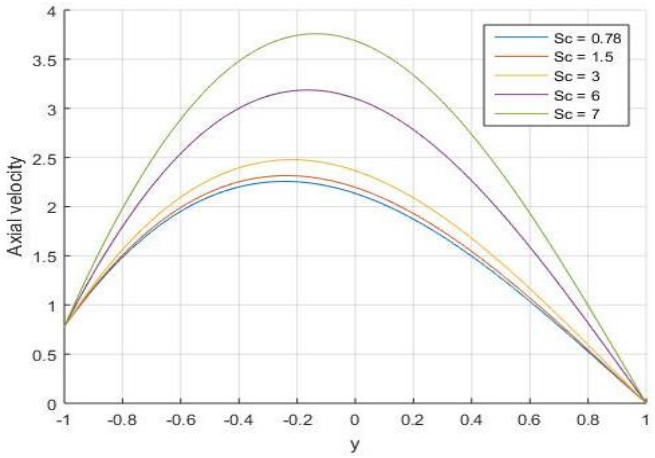

Figure 16. Velocity profile for different values of *Sc*

4.1.10 Axial Velocity for Different Values of Heat Source and Decay Parameter

Figure 16 illustrates the axial velocity distribution for various heat source parameter values (0.50, 0.75, 1.25, 1.50, 1.75) at λ=0.5, τ=0.5, *Pr*=1, *t*=1, *h*=0.5, *Ha*=1, *g*=9.81, β=0.5, β'=0.5, *Sc*=0.78, *Sr*=0.15. The observation indicates that axial velocity escalates as the heat source parameter (*S*) increases. Also, a noteworthy rise in blood velocity has been observed in figure 17 as the decay parameter decreases through (1.50,1.25,1.00,0.75,0.50) at constant μ=0.5, *Pr*=1, *S*=1, τ=0.5, *t*=1, *h*=0.5, *Ha*=1, *g*=9.81, β=0.5, β'=0.5, *Sc*=0.78, *Sr*=0.15.

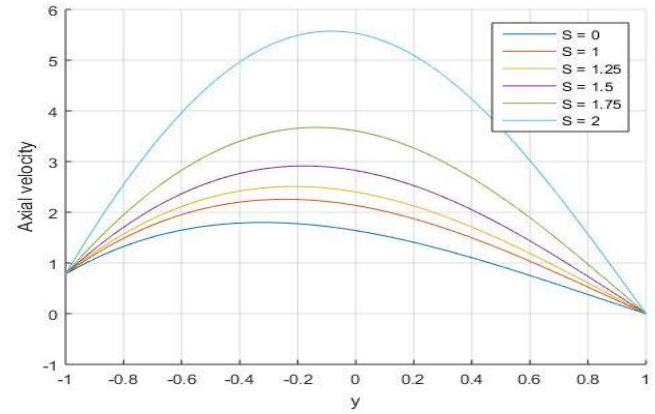

Figure 17. Velocity profile for different values of *S*

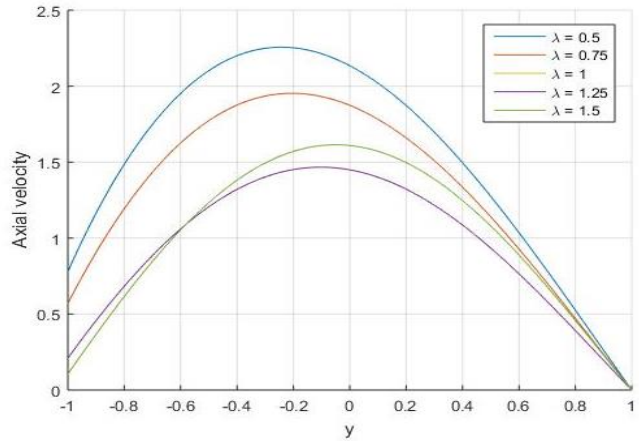

Figure 18. Velocity profile for different values of λ

4.1.11 Axial Velocity for Different Values of Hartmann Number and Time

In Figure 18, the influence of different Hartmann numbers (*Ha*) on axial velocity is evident. Notably, at *Ha*=1 and *Ha*=2, the velocity exhibits an increase from the left boundary towards the middle of the artery, followed by a subsequent decline. Conversely, at *Ha*=4 and *Ha*=6, the velocity experiences a sudden decrease towards *y*=−6 and then proceeds to decline gradually. This distinct trend highlights the sensitivity of axial velocity to variations in the Hartmann number, offering valuable insights into the complex dynamics of fluid flow under the influence of magnetic fields. The axial velocity pattern depicted in Figure 19 displays a consistent behavior over equal time intervals, indicating a steady and predictable evolution of the fluid flow. As time progresses, the temperature consistently changes by a constant amount during successive intervals, highlighting a proportional relationship between time and temperature variations. Notably, the most pronounced velocity is observed at the midpoint of the artery, suggesting a region of heightened fluid motion at this specific location over the course of time. This observation provides valuable insights into the dynamic and spatial aspects of fluid flow within the artery, contributing to our understanding of the overall flow patterns.

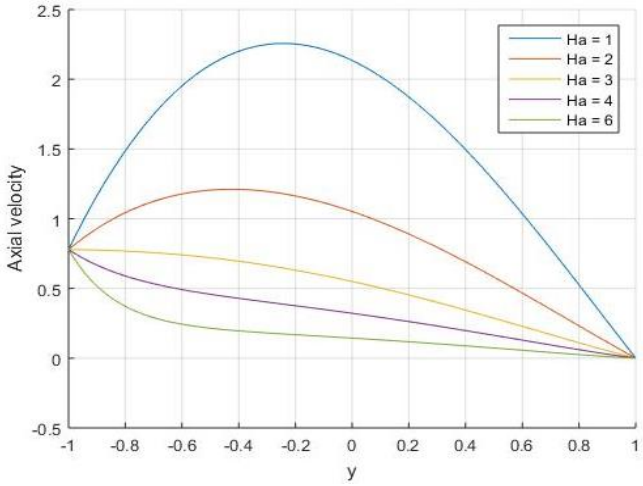

Figure 19. Velocity profile for different values of *Ha*

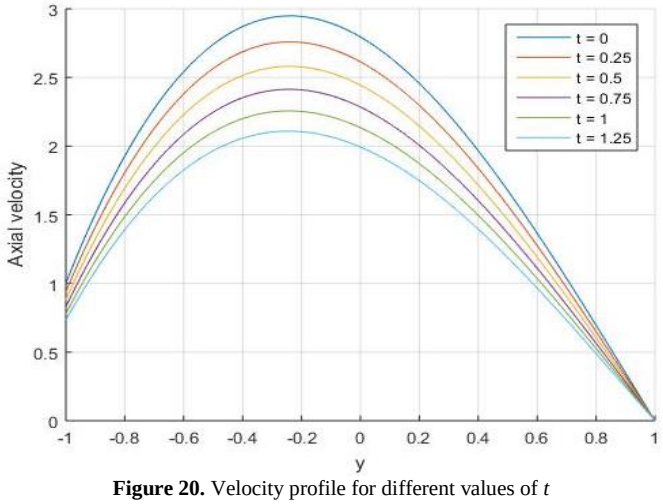

Figure 20. Velocity profile for different values of *t*

4.1.12 Normal Velocity for Different Values of Decay Parameter

Figure 20 shows how the decay parameter affects the distribution of normal velocity. It is demonstrated that when the decay parameter increases, the normal velocity falls. At low decay parameter values (0.50), the normal velocity falls slowly but at high decay parameter values (1.50), it decreases rapidly and leads to zero.

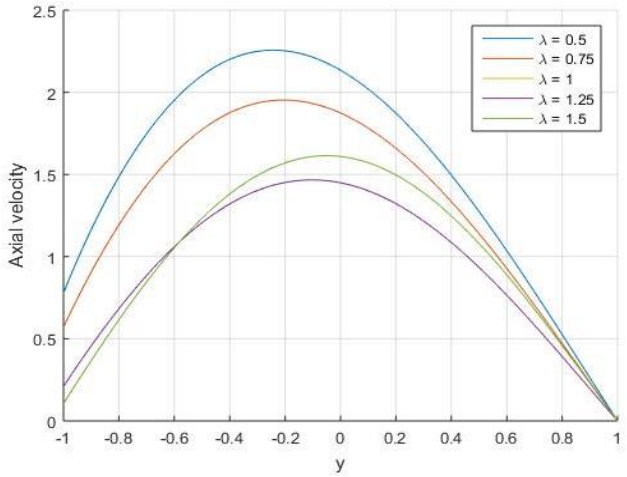

Figure 21. Normal velocity profile for different values of λ

5. Conclusion and Future Scope

This research investigates the unsteady blood flow through a bifurcated artery, incorporating the significant influence of the Soret effect and crucial factors such as heat source, magnetic field, Prandtl number and Schmidt number. The Soret effect, represented by the parameter *Sr*, emerges as a key player in altering concentration patterns and, consequently, blood velocity. As *Sr* decreases, a notable increase in blood velocity is observed, with a wide-ranging impact within specific *Sr* values. This emphasizes the importance of considering the Soret effect in understanding and predicting variations in blood flow dynamics, cardiovascular diseases and diseases that have abnormal blood circulation such as peripheral vascular disease and hypertension. The research, conveyed through graphical representations, contributes valuable insights into the complex interplay of parameters and their effects on blood behavior, particularly shedding light on the pivotal role of the Soret effect in influencing blood flow characteristics.

Data Availability

The authors declare that the data supporting the findings of this study are available within the paper.

Conflict of Interest

On behalf of all authors, the corresponding author states that there is no conflict of interest.

Funding Source

There is no funding for this research

Authors' Contributions

All authors contributed equally.

Acknowledgements

We are deeply thankful to our patient, supportive, and inspiring mentor, Dr. Yusuf Ya'u Gambo, who guided us in achieving our goal of establishing a strong foundation in Bio-Fluid Dynamics.

References

[1] E. E. Tzirtzilakis, "A Mathematical Model for Blood Flow in Magnetic Field", *Journal of Physics of Fluids*, Vol. **17**, Issue **7**, pp. **07-11, 2005.**

[2] G. Ramamurthy, B. Shanker, "Magnetohydrodynamic Effects on Blood Flow through Porous Channel", Journal of *Medical and Biological Engineering and Computing*, Vol. 32, Issue 6, pp. **655-659, 1994.**

[3] K. Das, G. C. Saha, "Arterial MHD Pulsatile Flow of Blood under Periodic Body Acceleration", *Bulletin of Society of Mathematicians Banja Luka*, Vol. **16**, No. **1**, pp. **21-42, 2009.**

[4] M. E. Islam, "Mathematical Analysis of Unsteady MHD Blood Flow through Parallel Plate Channel with Heat Source", *World Journal of Mechanics* , Vol. **2**, Issue **3**, pp. **131-137, 2012.**

[5] J. Singh, R. Rathee, "Analytical Solution of Two- Dimensional Model of Blood Flow with Variable Viscosity through an Indented Artery Due to LDL Effect in the Presence of Magnetic Field", *International Journal of Physical Sciences*, Vol. 5, Issue 12, pp. **1857-1868, 2010.**

[6] C. S. Dulal, B. Ananda, "Pulsatile Motion of Blood through an AxiSymmetric Artery in Presence of Magnetic Field", *Journal of Science and Technology of Assam University*, Vol. 5, Issue 2, pp. **12-20, 2010.**

[7] M. Zamir, M. R. Roach, "Blood flow downstream of a two dimensional bifurcation" , *Journal of Theoretical Biology, Vol. 5,* Issue *6, pp.* **33-42, 1973.**

[8] A. Kolin, "An electromagnetic flow meter: Principle of the method and its application to blood flow measurements", *Proc. Soc. exp. Biol.* (N. Y.), Vol. 6, Issue 35, pp. **53-56, 1936.**

[9] E. M. Korchevskii, L. S. Marochnik, "Magnetohydrodynamic version of movement of blood", Journal of *Biophysics*, Vol. 12, Issue 10, pp. **411-413, 1965.**

[10] M. Usman, S. Tauseef, D. Mohyud, "Fluid flow and heat transfer investigation of blood with nanoparticles through porous vessels in the presence of magnetic field", *Journal of Algorithm Computing Technol*ogy, Vol. 11, Issue 13, pp. **1-15, 2008.**

[11] D. A. A. Tripathy, "Mathematical model for blood flow through inclined arteries under the influence of inclined magnetic field", *Journal of Medical Biology, Vol. 11, No. 12, pp. 1-16, 2012.*

[12] M. J. Allwood, H. S. Burry, "The effect of local temperature on blood flow in human foot", *Journal of Physiology , Vol. 124,* Issue *2, pp. 133-357,* **1954.**

[13] A. Ogulu, T. M. Abbey, "Simulation of heat transfer on an oscillatory blood flowin an indented porous artery", *International Journal of communication in heat and mass transfer*, Vol 32, Issue 5, pp. **983-989, 2005.**

[14] H. S. Burry, M. J. Allwood, "*The effect of local temperature on blood flow in the human foot"* , Journal of Human Physiology, Vol. 15, Issue 2, pp. **45-51,1954.**

[15] S. Charm, B. Paltiel, G. S. Kurland, "*Heat transfer coefficients in blood flow"*, Journal of Biorheology, Vol. **5**, Issue **6**, pp.**133-145, 1968.**

[16] S. A. Victor, V. L. Shah, "*Heat transfer to blood flowing in a tube"*, Journal of Biorheology, Vol. **12**, Issue **11**, pp. **361-368, 1975.**

[17] K. Halder, "Effects of magnetic field on blood flow through an indented tube in the presence of erythrocytes", *Indian Journal of Pure and Applied Mathe*matics, Vol. 10, Issue 52, pp. **253-345, 1994.**

[18] V. A. Vardanyan, " The effects of fluid mechanics of human biotheuraptic Anatomy", Journal of *Biophysics, Vol. 7,* Issue 15, pp. **18-515, 1973.**

[19] G. Varshney, V. K. Katiyar, S. Kumar, "Effect of magnetic field on the blood flow in artery having multiple stenosis: a numerical study", *International Journal of Engineering Science Technology, Vol. 11,* Issue 2, pp. **67-82, 2010.**

[20] B. K. Jha, Y. Y. Gambo, "Unsteady free convection and mass transfer fow past an impulsively started vertical plate with Soret and Dufour efects: an analytical approach", Journal of *Applied Science, Vol 5,* Issue 1, pp. **12-34, 2019.**

[21] B. K. Jha, Y. Y. Gambo, "Dufour Effect with Ramped Wall Temperature and Specie Concentration on Natural Convection Flow through a Channel", Journal of Physics, Vol. 11, Issue 1, pp. **1-11, 2019.**

[22] B. K. Jha, Y. Y. Gambo, "Transient natural convention heat and mass transfer flow in a vertical channel in the presence of Soret and Dufour effects: An analytical approach", *International Journal of Modern Physics, Vol. 10,* Issue 31, pp. **2-9, 2020.**

[23] B. K. Jha, Y. Y. Gambo, "Soret and Dufour effects on transient free convention heat and mass transfer flow in a vertical channel with ramped wall temperature and specie concentration: an analytical approach", *Arab Journal of Basic and Applied Sciences, Vol. 7,* Issue, pp.**1-8, 2020.**

[24] B. Y. Isah, B. K. Jha, L. Jeng-Eng, "Combined effects of thermal diffusion and diffusion-thermo effects on transient MHD natural convection and mass transfer flow in a vertical channel with thermal radiation", Journal of *Applied Mathematics, Vol. 11,* Issue**,** pp.**23-54, 2016.**

AUTHORS PROFILE

Auwalu Alhassan Girema earned his Bsc Mathematics at the prestigious Ahmadu Bello University, Zaria-Nigeria. He is currently currently a student of Yusuf Maitama Sule university, Kano, Nigeria .

Yusuf Ya'u Gambo earned his Bsc in Bayaro University Kano-Nigeria., and Ph.D. prestigious Ahmadu Bello University, Zaria-Nigeria. He is currently working as Lecturer in Department of Mathematics, Yusuf Maitama Sule University, Kano, Nigeria

Bashir Yau Haruna earned his BSc at Alqalam University, Katsina-Nigeria He is currently currently a student of Yusuf Maitama Sule university, Kano, Nigeria.